Computer Assisted Mechanics and Engineering Sciences, 6: 439–447, 1999.

Numerical model of heat transfer between blood vessel and biological tissue

Ewa Majchrzak
Department for Strength of Materials and Computational Mechanics
Silesian Technical University, Konarskiego 18a, 44-100 Gliwice, Poland

Bohdan Mochnacki
Institute of Mathematics and Computer Science
Technical University of Częstochowa, Dąbrowskiego 73, 42-200 Częstochowa, Poland

(Received March 8, 1999)

The thermal processes proceeding within a perfused tissue in the presence of a vessel are considered. The Pennes bio-heat transfer equation determines the steady state temperature field in tissue sub-domain, while the ordinary differential equation resulting from the energy balance describes the change of blood temperature along the vessel. The coupling of above equations results from the boundary condition given on the blood vessel wall. The problem is solved using the combined numerical algorithm, in particular the boundary element method (for the tissue sub-domain) and the finite differences method (for blood vessel sub-domain).

1. Introduction

The heat transfer processes proceeding in a domain of biological tissue are described by the Pennes equation. If one considers the steady state problem then this equation takes a form

$$\operatorname{div}\left[\lambda(T)\operatorname{grad}T(X)\right] + Q_{\text{met}} + c_b\, G_b\left[T_b(X) - T(X)\right] = 0 \tag{1}$$

where λ is the tissue thermal conductivity, c_b is the specific heat of blood (per unit of volume), G_b [m^3 blood /s/m^3 tissue] is the tissue perfusion, Q_{met} is the metabolic heat source, T, X denote the temperature and spatial co-ordinates. The last term in Eq. (1) is called the perfusion heat source (Q_{perf}).

The Pennes bio-heat transfer equation has the essential limitation that it cannot to simulate the effects of large, widely spaced thermally significant blood vessel [6]. So, in literature [5, 6, 7] one can find the models being the composition of the bio-heat transfer equation and the another equation describing the behavior of blood vessel. In this paper the energy equation concerning the blood vessel results from the energy balance for the fragment distinguished in sub-domain considered (see Section 2). The similar equations are presented among others in [5, 6, 9]. The problem is treated as the 2D axially symmetrical one. The coupling of the Pennes and the blood vessel energy equations results from the continuity of heat flux on the vessel wall. In order to solve the problem the numerical methods are used, in particular the boundary element method for the tissue sub-domain and the finite differences method for the blood sub-domain. In the final part of the paper the results of numerical simulations are presented.

2. GOVERNING EQUATIONS

A single large blood vessel embedded in a perfused tissue is considered. The non-homogeneous vessel–tissue domain is oriented in cylindrical co-ordinate system as in Fig. 1, and the steady state problem is considered.

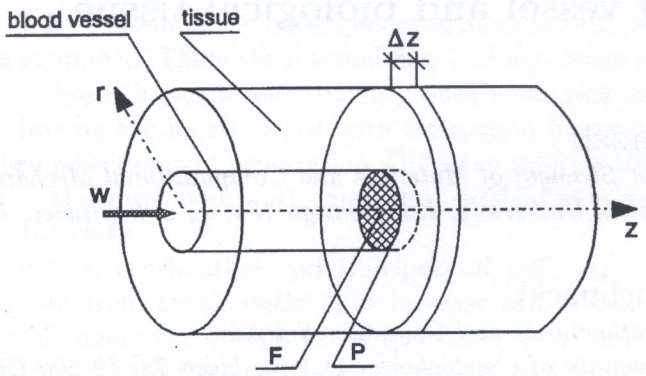

Fig. 1. Non-homogeneous domain blood vessel–tissue

Additionally, it is assumed that the temperature of blood corresponding to co-ordinate z is uniform, this means $T_b(r,z) = T_b(z)$. The energy balance for the volume $F\Delta z$ can be written in the form

$$H(z) = H(z+\Delta z) + Q_0 \tag{2}$$

where $H(z)$ is the blood enthalpy at point z, $H(z+\Delta z)$ is the blood enthalpy at point $z+\Delta z$, Q_0 is the heat flowing between blood and tissue. So

$$H(z) = w\,F\,c_b\,T_b(z) \tag{3}$$

and

$$H(z+\Delta z) = w\,F\,c_b\,T_b(z) + \frac{\mathrm{d}}{\mathrm{d}z}\left[w\,F\,c_b\,T_b(z)\right]\Delta z \tag{4}$$

while

$$Q_0 = \alpha\,P\Delta z\,\left[T_b(z) - T(r_1,z)\right]\,. \tag{5}$$

In above formulas w is the blood velocity, F is the vessel lateral section, P is the vessel periphery, α is the heat transfer coefficient between blood and tissue, $T(r_1,z)$ is the vessel wall temperature.

The energy balance (2) for constant values of w, c_b, F and P leads to the following differential equation

$$c_b\,w\,F\,\frac{\mathrm{d}\,T_b(z)}{\mathrm{d}z} + \alpha\,P\,\left[T_b(z) - T(r_1,z)\right] = 0 \tag{6}$$

at the same time for $z=0$: $T_b(0) = T_{b0}$.

The Pennes bio-heat transfer equation describing the steady temperature field in the tissue subdomain is of the form

$$\frac{1}{r}\,\frac{\partial}{\partial r}\left[r\,\lambda\,\frac{\partial T(r,z)}{\partial r}\right] + \frac{\partial}{\partial z}\left[\lambda\,\frac{\partial T(r,z)}{\partial z}\right] + Q_{\mathrm{perf}} + Q_{\mathrm{met}} = 0. \tag{7}$$

In this paper, the terms Q_{met} and Q_{perf} according to [5] are assumed as the constant values. Considering the more complex model, the change of $T_b(z)$ in the formula determining Q_{perf} should

be taken into account. The algorithm presented in this paper allows to find the solution in which the change of Q_{perf} is considered, for instance the simple iterative procedure can be introduced.

Equation (7) is supplemented by the following boundary conditions — c.f. Fig. 2

$$\begin{cases} r = r_1: & q(r,z) = \alpha\,[T(r,z) - T_b(z)] \\ r = r_2: & T(r,z) = T^{\infty} \\ z = 0: & q(r,z) = 0 \\ z = Z: & q(r,z) = 0 \end{cases} \tag{8}$$

where r_1 is the vessel radius, r_2 is the arbitrary assumed external radius of biological tissue, $q(r,z)$ is the normal heat flux ($q = -\lambda \partial T/\partial n$), T^{∞} is the boundary tissue temperature.

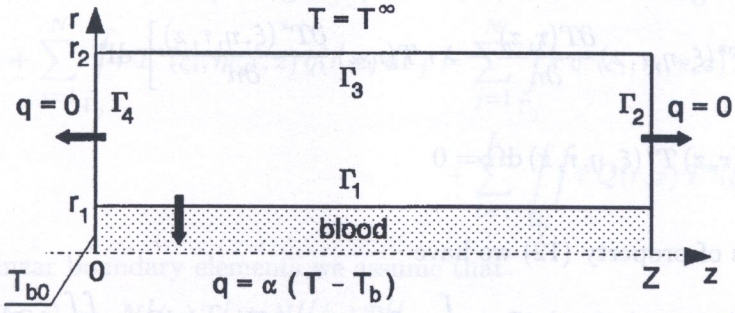

Fig. 2. Domain considered

3. THE BOUNDARY ELEMENT METHOD FOR CYLINDRICAL SHELL

Let us assume, that $Q(r,z) = Q_{\text{met}} + Q_{\text{perf}}$ and the tissue thermal conductivity is a constant value. So the following Pennes equation is considered

$$\lambda \frac{\partial}{\partial r}\left[r \frac{\partial T(r,z)}{\partial r}\right] + \lambda \frac{\partial}{\partial z}\left[r \frac{\partial T(r,z)}{\partial z}\right] + r\,Q(r,z) = 0\,. \tag{9}$$

Application of the weighted residual formulation [3, 4, 8] leads to the following formula

$$\iint_{\Omega} \left\{\lambda \frac{\partial}{\partial r}\left[r \frac{\partial T(r,z)}{\partial r}\right] + \lambda \frac{\partial}{\partial z}\left[r \frac{\partial T(r,z)}{\partial z}\right] + r\,Q(r,z)\right\} T^*(\xi,\eta,r,z)\,\mathrm{d}\Omega = 0 \tag{10}$$

where Ω is the domain of tissue, $T^*(\xi,\eta,r,z)$ is the fundamental solution, while $(\xi,\eta) \in \Omega$ is the observation point. The fundamental solution for the problem considered is of the form [2, 3, 4]

$$T^*(\xi,\eta,r,z) = \frac{1}{\lambda\pi\sqrt{(r+\xi)^2 + (z-\eta)^2}}\,K(m)\,, \qquad m = \frac{4r\xi}{(r+\xi)^2 + (z-\eta)^2}\,, \tag{11}$$

where $K(\cdot)$ is the elliptic integral of the first type [1].

The function $T^*(\xi,\eta,r,z)$ fulfills the following equation

$$\lambda \frac{\partial}{\partial r}\left[r \frac{\partial T^*(\xi,\eta,r,z)}{\partial r}\right] + \lambda \frac{\partial}{\partial z}\left[r \frac{\partial T^*(\xi,\eta,r,z)}{\partial z}\right] = -\delta(\xi,\eta,r,z) \tag{12}$$

where $\delta(\xi,\eta,r,z)$ is the Dirac function and it has the following property

$$\delta(\xi,\eta,r,z) = \begin{cases} 0\,, & (\xi,\eta) \neq (r,z) \\ \infty\,, & (\xi,\eta) = (r,z) \end{cases} \tag{13}$$

The weighted residual criterion (10) can be written in the form

$$\iint_{\Omega} \left\{ \lambda \frac{\partial}{\partial r}\left[r \frac{\partial T(r,z)}{\partial r} \right] + \lambda \frac{\partial}{\partial z}\left[r \frac{\partial T(r,z)}{\partial z} \right] \right\} T^*(\xi,\eta,r,z)\, \mathrm{d}\Omega + \iint_{\Omega} r\, Q(r,z)\, T^*(\xi,\eta,r,z)\, \mathrm{d}\Omega = 0 \tag{14}$$

Using the second Green formula [8] to the first component of above equation one obtains

$$\iint_{\Omega} \left\{ \lambda \frac{\partial}{\partial r}\left[r \frac{\partial T^*(\xi,\eta,r,z)}{\partial r} \right] + \lambda \frac{\partial}{\partial z}\left[r \frac{\partial T^*(\xi,\eta,r,z)}{\partial z} \right] \right\} T(r,z)\, \mathrm{d}\Omega + \int_{\Gamma} \left[\lambda r\, T^*(\xi,\eta,r,z) \frac{\partial T(r,z)}{\partial n} - \lambda r\, T(r,z) \frac{\partial T^*(\xi,\eta,r,z)}{\partial n} \right] \mathrm{d}\Gamma + \iint_{\Omega} r\, Q(r,z)\, T^*(\xi,\eta,r,z)\, \mathrm{d}\Omega = 0 \tag{15}$$

Finally, on the basis of property (12) we have

$$T(\xi,\eta) + \int_{\Gamma} r\, T^*(\xi,\eta,r,z)\, q(r,z)\, \mathrm{d}\Gamma = \int_{\Gamma} r\, q^*(\xi,\eta,r,z)\, T(r,z)\, \mathrm{d}\Gamma + \iint_{\Omega} r\, Q(r,z)\, T^*(\xi,\eta,r,z)\, \mathrm{d}\Omega. \tag{16}$$

One can notice, that in the above equation $q(r,z) = -\lambda \partial T(r,z)/\partial n$, while $q^*(\xi,\eta,r,z) = -\lambda\, \partial T^*(\xi,\eta,r,z)/\partial n$. The heat flux $q^*(\xi,\eta,r,z)$ is equal to

$$q^*(\xi,\eta,r,z) = \frac{1}{\pi\sqrt{(r+\xi)^2 + (z-\eta)^2}} \left\{ \frac{1}{2r} \left[K(m) - \frac{\xi^2 - r^2 + (z-\eta)^2}{(r-\xi)^2 + (z-\eta)^2} E(m) \right] \cos\alpha_r + \frac{z-\eta}{(r-\xi)^2 + (z-\eta)^2} E(m) \cos\alpha_z \right\} \tag{17}$$

where $E(\cdot)$ is the elliptic integral of the second type [1], $\cos\alpha_r$, $\cos\alpha_z$ are the directional cosines of normal versor n at the boundary point (r,z).

It should be pointed out that in numerical realization the values of functions $K(\cdot)$ and $E(\cdot)$ are calculated on the basis of approximate formulas presented among others in [1]. For $(\xi,\eta) \in \Gamma$ Eq. (16) takes a form

$$B(\xi,\eta)\, T(\xi,\eta) + \int_{\Gamma} r\, T^*(\xi,\eta,r,z)\, q(r,z)\, \mathrm{d}\Gamma = \int_{\Gamma} r\, q^*(\xi,\eta,r,z)\, T(r,z)\, \mathrm{d}\Gamma + \iint_{\Omega} r\, Q(r,z)\, T^*(\xi,\eta,r,z)\, \mathrm{d}\Omega\,. \tag{18}$$

The coefficient $B(\xi,\eta)$ is a number from the scope (0, 1) [3, 4].

4. Numerical model

At first, the problem of temperature field computations in tissue sub-domain will be discussed. So, we divide the boundary Γ into N linear boundary elements, while the interior Ω into L linear internal cells — Fig. 3.

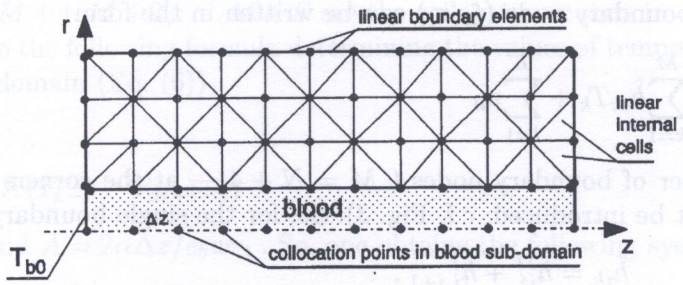

Fig. 3. Discretization

The discrete form of the boundary integral equation (18) is the following

$$B(\xi_i,\eta_i)\,T(\xi_i,\eta_i)+\sum_{j=1}^{N}\int\limits_{\Gamma_j} r\,T^*(\xi_i,\eta_i,r,z)\,q(r,z)\,\mathrm{d}\Gamma_j=\sum_{j=1}^{N}\int\limits_{\Gamma_j} r\,q^*(\xi_i,\eta_i,r,z)\,T(r,z)\,\mathrm{d}\Gamma_j + \sum_{l=1}^{L}\iint\limits_{\Omega_l} r\,Q(r,z)\,T^*(\xi_i,\eta_i,r,z)\,\mathrm{d}\Omega_l\,. \tag{19}$$

For the case of linear boundary elements we assume that

$$(r,z)\in\Gamma_j:\begin{cases} T(r,z) &= N_j^I(u)\,T_j^I+N_j^{II}(u)\,T_j^{II}\\ q(r,z) &= N_j^I(u)\,q_j^I+N_j^{II}(u)\,q_j^{II}\end{cases} \tag{20}$$

where

$$N_j^I(u)=(1-u)/2,\qquad N_j^{II}(u)=(1+u)/2,\qquad u\in[-1,1]$$

are the shape functions, $T_j^I=T(r_I,z_I)$, $T_j^{II}=T(r_{II},z_{II})$, etc., are the temperatures and heat fluxes corresponding to the limits of the element considered. So

$$\int\limits_{\Gamma_j} r\,q^*(\xi_i,\eta_i,r,z)\,T(r,z)\,\mathrm{d}\Gamma_j=h_{ij}^I T_j^I+h_{ij}^{II}\,T_j^{II} \tag{21}$$

and

$$\int\limits_{\Gamma_j} r\,T^*(\xi_i,\eta_i,r,z)\,q(r,z)\,\mathrm{d}\Gamma_j=g_{ij}^I\,q_j^I+g_{ij}^{II}\,q_j^{II} \tag{22}$$

where

$$h_{ij}^I=\frac{l_j}{2}\int_{-1}^{1} N_j^I(N_j^I r_I+N_j^{II}r_{II})\,q^*(\xi_i,\eta_i,N_j^I r_I+N_j^{II}r_{II},N_j^I z_I+N_j^{II}z_{II})\,\mathrm{d}u\,, \tag{23}$$

$$h_{ij}^{II}=\frac{l_j}{2}\int_{-1}^{1} N_j^{II}(N_j^I r_I+N_j^{II}r_{II})\,q^*(\xi_i,\eta_i,N_j^I r_I+N_j^{II}r_{II},N_j^I z_I+N_j^{II}z_{II})\,\mathrm{d}u\,, \tag{24}$$

$$g_{ij}^I=\frac{l_j}{2}\int_{-1}^{1} N_j^I(N_j^I r_I+N_j^{II}r_{II})\,T^*(\xi_i,\eta_i,N_j^I r_I+N_j^{II}r_{II},N_j^I z_I+N_j^{II}z_{II})\,\mathrm{d}u\,, \tag{25}$$

$$g_{ij}^{II}=\frac{l_j}{2}\int_{-1}^{1} N_j^{II}(N_j^I r_I+N_j^{II}r_{II})\,T^*(\xi_i,\eta_i,N_j^I r_I+N_j^{II}r_{II},N_j^I z_I+N_j^{II}z_{II})\,\mathrm{d}u\,. \tag{26}$$

In formulas (23)–(26) l_j is the length of element Γ_j.

Equation (19) for boundary node (ξ_i, η_i) can be written in the form

$$B_i T_i + \sum_{k=1}^{M} g_{ik} q_k = \sum_{k=1}^{M} \hat{h}_{ik} T_k + \sum_{l=1}^{L} p_{il} \tag{27}$$

where M is the number of boundary nodes ($M = N + 4$ — at the corners of domain considered the double nodes must be introduced, c.f. Fig. 3). So, for the single boundary node k we have

$$g_{ik} = g_{ij}^{II} + g_{i,j+1}^{I}\,, \qquad \hat{h}_{ik} = h_{ij}^{II} + h_{i,j+1}^{I}\,, \tag{28}$$

while for the double boundary node $k, k+1$

$$\begin{aligned} g_{ik} &= g_{ij}^{II}\,, \qquad g_{i,k+1} = g_{i,j+1}^{I}\,, \\ \hat{h}_{ik} &= h_{ij}^{II}\,, \qquad \hat{h}_{i,k+1} = h_{i,j+1}^{I}\,, \end{aligned} \tag{29}$$

The values p_{il} in Eq. (27) are equal to

$$p_{il} = \iint_{\Omega_l} r\, Q(r,z)\, T^*(\xi_i, \eta_i, r, z)\, \mathrm{d}\Omega_l\,. \tag{30}$$

Assuming the linear approximation of source function $Q(r,z)$:

$$(r,z) \in \Omega_l: \qquad Q(r,z) = N_l^I Q(r_I, z_I) + N_l^{II} Q(r_{II}, z_{II}) + N_l^{III} Q(r_{III}, z_{III}), \tag{31}$$

where N_l^I, N_l^{II}, N_l^{III} are the 2D linear shape functions [8], one can find the values of p_{il} using the typical methods of numerical integration [4]. The problem is not complex because the integrand in Eq. (30) is known.

One can write Eq. (27) for each 'i' node, obtaining M equations

$$\sum_{k=1}^{M} g_{ik} q_k = \sum_{k=1}^{M} h_{ik} T_k + \sum_{l=1}^{L} p_{il} \tag{32}$$

where [3]

$$h_{ik} = \begin{cases} \hat{h}_{ik}\,, & i \neq k, \\ -B_i = -\sum\limits_{k \neq i} \hat{h}_{ik}\,, & i = k. \end{cases} \tag{33}$$

For the needs of further considerations the equations concerning the nodes on the boundary Γ_1 (Fig. 4) are considered seperately. So

$$\sum_{k=1}^{S} g_{ik}\, q_k + \sum_{k=S+1}^{M} g_{ik}\, q_k = \sum_{k=1}^{M} h_{ik}\, T_k + \sum_{l=1}^{L} p_{il} \tag{34}$$

where S is the number of nodes corresponding to Γ_1.

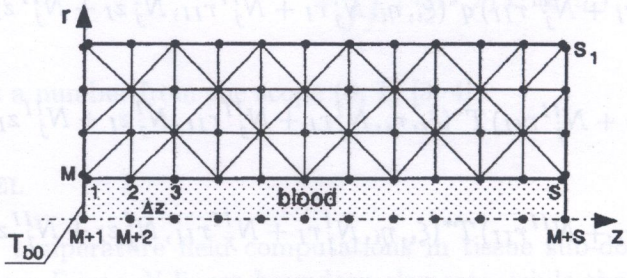

Fig. 4. The coupling of sub-domains

Let us assume that $M+1, M+2, \ldots, M+S$ are the collocation points in domain of blood. The FDM algorithm leads to the following formula determining the values of temperatures at collocation points from the blood domain (Eq. (6))

$$\begin{aligned} T_{M+1} &= T_{b0} \\ T_{M+k} &= T_{M+k-1} + A\,(T_{k-1} - T_{M+k-1}) \end{aligned} \tag{35}$$

where $k = 2, 3, \ldots, S$ and $A = 2\alpha\Delta z / c_b w r_1$. So, one obtains the following system of equations

$$\begin{cases} \sum\limits_{k=1}^{S} g_{ik}\,\alpha\,(T_k - T_{M+k}) + \sum\limits_{k=S+1}^{M} g_{ik}\,q_k = \sum\limits_{k=1}^{M} h_{ik}\,T_k + \sum\limits_{l=1}^{L} p_{il}\,, \qquad i = 1, \ldots, M, \\ T_{M+1} = T_{b0}\,, \\ AT_{k-1} + (1-A)\,T_{M+k-1} - T_{M+k} = 0, \qquad k = 2, 3, \ldots, S\,. \end{cases} \tag{36}$$

Taking into account the boundary conditions given on the boundaries Γ_2, Γ_3 and Γ_4 (Fig. 2) we have the well-ordered form of the system (36)

$$\begin{cases} \sum\limits_{k=1}^{S} (\alpha\, g_{ik} - h_{ik})\,T_k - \sum\limits_{k=S+1}^{S_1} h_{ik}\,T_k + \sum\limits_{k=S_1+1}^{S_1+S} g_{ik}\,q_k \\ \qquad - \sum\limits_{k=S_1+S+1}^{M} h_{ik}\,T_k - \sum\limits_{k=M+1}^{M+S} \alpha\, g_{i,k-M}\,T_k = \sum\limits_{k=S_1+1}^{S_1+S} h_{ik}\,T^{\infty} + \sum\limits_{l=1}^{L} p_{il}\,, \quad i = 1, \ldots, M, \\ T_{M+1} = T_{b0}\,, \\ AT_{i-M-1} + (1-A)\,T_{i-1} - T_i = 0, \qquad i = M+2, M+3, \ldots, M+S\,, \end{cases} \tag{37}$$

where index S_1 is shown in Fig. 4.

After solution of the above system of equations, all boundary temperatures and heat fluxes for tissue sub-domain are known and next one can find the internal temperatures at the points $(\xi_i, \eta_i) \in \Omega$ using the equation

$$T_i = \sum_{k=1}^{M} h_{ik}\,T_k - \sum_{k=1}^{M} g_{ik}\,q_k + \sum_{l=1}^{L} p_{il}\,. \tag{38}$$

5. The results of computations

The blood vessel of radius $r_1 = 0.0005\,[\mathrm{m}]$ is considered. The external radius of domain is assumed as $r_2 = 10 r_1$ while $Z = 0.021\,[\mathrm{m}]$ (Fig. 2). The following input data are take into account [5, 6]: $\lambda = 0.5\,[\mathrm{W/mK}]$, $Q_{\mathrm{met}} = 245\,[\mathrm{W/m^3}]$, $Q_{\mathrm{perf}} = 10^4\,[\mathrm{W/m^3}]$, $c_b = 4.134{\cdot}10^6\,[\mathrm{J/m^3\,K}]$, $w = 0.08\,[\mathrm{m/s}]$, $P/F = 2/r_1 = 4000\,[1/\mathrm{m}]$, the Nusselt number $\mathrm{Nu} = \alpha\, 2 r_1/\lambda = 4$ ($\alpha = 2000\,[\mathrm{W/m^2K}]$). It should

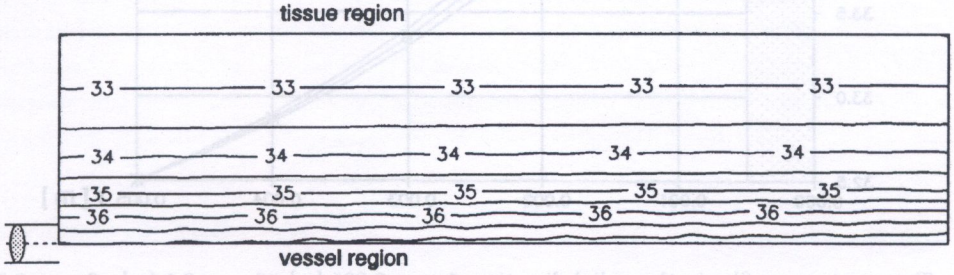

Fig. 5. Temperature field in the domain considered

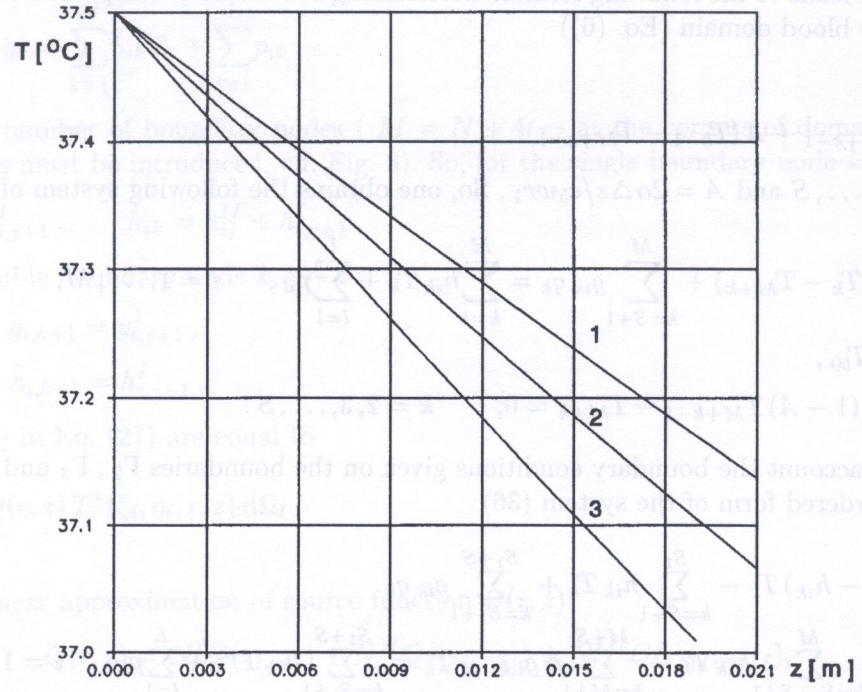

Fig. 6. Blood temperature along the vessel; 1: $w = 0.1$ [m/s], Nu $= 4$, 2: $w = 0.08$ [m/s], Nu $= 4$, 3: $w = 0.06$ [m/s], Nu $= 4$

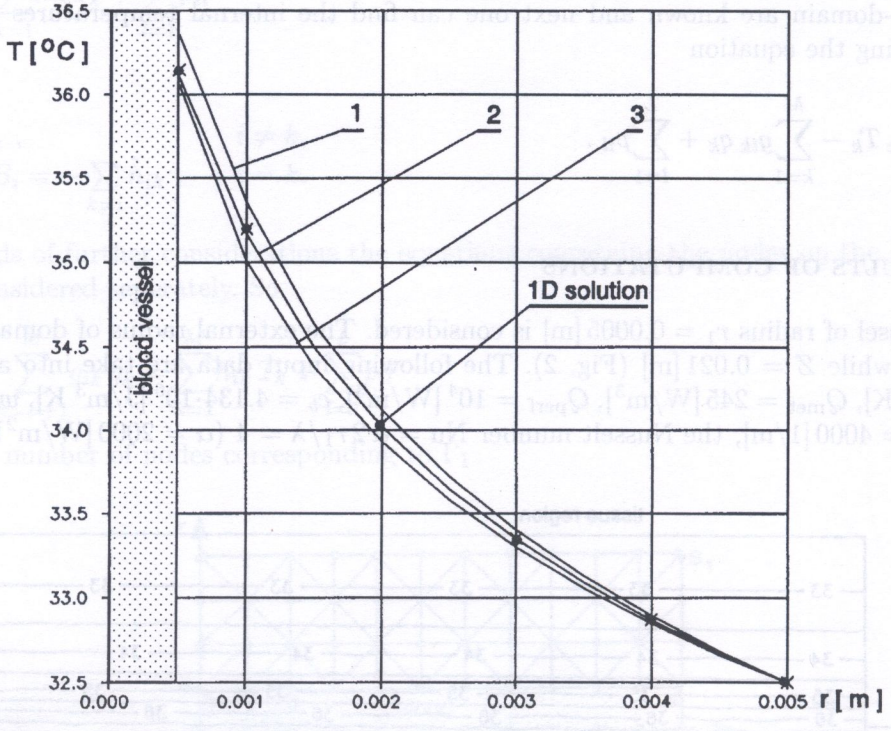

Fig. 7. Temperature profiles in the radial direction; 1: $z = 0.005$ [m], 2: $z = 0.1$ [m], 3: $z = 0.21$ [m]

be pointed out that the algorithm presented allows to consider the problem for which $Q_{\text{perf}} = Q_{\text{perf}}(r, z)$.

The boundary of tissue has been divided into $N = 60$ linear boundary elements ($M = 64$), while the interior has been divided into $L = 370$ linear triangular internal cells. The number of collocation points along the blood vessel: $S = 22$.

In Fig. 5 the temperature field in domain analyzed is shown. The successive isotherms are nearly parallel but the effect of thermal interactions between blood vessel and tissue is visible.

Figure 6 presents the change of blood temperature along the vessel for different rates of blood, while in Fig. 7 the temperature profiles in the tissue sub-domain for $z = 0.005$, 0.1 and 0.21 [m] are marked. A certain way of the verification of results can be the comparison of profiles obtained with the 1D analytical solution for cylindrical shell (the Dirichlet conditions for $r = r_1$ and $r = r_2$ are assumed). The solution corresponding to $z = 0.1$ [m] is also shown in Fig. 7.

It should be pointed out, that taking into account the simple geometry of non-homogeneous domain considered, the others methods of numerical computations of temperature field in domain of tissue can be also applied. The main advantage of the BEM application results from the fact, that the final system of equations concerns only the boundary nodes and the number of unknown parameters is essentially smaller than in the case of the finite differences method or the finite element method. Additionally, the BEM assures the good approximation of boundary conditions.

ACKNOWLEDGEMENT

This paper is a part of project No 8 T11F 016 13 sponsored by KBN.

REFERENCES

[1] M. Abramowitz, I.A. Stegun. *Handbook of mathematical functions.* Dover Publications, Inc., New York, 1985.

[2] R. Białecki, A. Nowak, R. Nahlik. Application of axially symmetrical fundamental solution and Green's function in the BEM (in Polish). In: *Proceedings of the Conference Modelling in Mechanics.* PTMTiS, Gliwice, 29–36, 1982.

[3] C.A. Brebbia, J. Dominiguez. *Boundary Elements – An Introductory Course.* Comp. Mech. Publications and Mc Graw–Hill Book Co., Southampton and Boston, 1992.

[4] C.A. Brebbia, J.C.F. Telles, L.C. Wrobel. *Boundary Element Techniques.* Springer-Verlag, Berlin–Heidelberg–New York, Tokyo, 1984.

[5] H. Brinck, J. Werner. Estimation of the thermal effect of blood flow in a branching countercurrent network using a three-dimensional vascular model. *Journal of Biomechanical Engineering, Transactions of the ASME*, **116**: 324–330, 1994.

[6] H.W. Huang, C.L. Chan, R.B. Roemer. Analytical solutions of Pennes bio-heat transfer equation with a blood vessel. *Journal of Biomechanical Engineering, Transactions of the ASME*, **116**: 208–212, 1994.

[7] H.W. Huang, Z.P. Chen, R.B. Roemer. A counter current vascular network model of heat transfer in tissues. *Journal of Biomechanical Engineering, Transactions of the ASME*, **118**: 120–129, 1996.

[8] E. Majchrzak. *Application of the BEM in the thermal theory of foundry* (in Polish). Publ. of the Silesian Technical University, Mechanics, **102**, Gliwice, 1991.

[9] L. Zhu, S. Weinbaum. A model for heat transfer from embedded blood vessels in two-dimensional tissue preparations. *Journal of Biomechanical Engineering, Transactions of the ASME*, **117**: 64–73, 1995.